
Research on Fiber Placement Trajectory Design Algorithm for the Free-Form Surface With Given Ply Orientation Information

Wang Peiyuan*, Li Yong, Wang Xianfeng, and Xiao Jun

(College of Material Science and Technology, Nanjing University of Aeronautics and Astronautics, Nanjing 210016, China)

SUMMARY

Aiming at the traditional fixed-angle trajectory design methods in automatic composite fiber placement, a novel trajectory design algorithm based on given ply orientation information of the free-form surface is proposed. Firstly, the initial reference path is constructed with the given points and modified fiber-placement directions that are calculated by weighted average algorithm. Then, “feature section” method is carried out to solve the full-spreadability issue and all other center paths are generated by the parallel equidistant path generation method based on geodesic theory of the classic differential geometry. Finally, the Newton–Raphson iteration algorithm is applied to solve the intersection issue between fiber path and boundary, which can realize the integrated placement at the boundary area. Based on the above algorithms, the CAD module of the trajectory planning for the free-form surface with given ply orientation information is developed with the environment of CATIA V5R18, and is validated by simulations. The results show that the above algorithms can accomplish the trajectory design based on the ply orientation information and make a positive exploration on the variable angle trajectory design in automatic fiber placement.

1. INTRODUCTION

As a new cost-effective automated manufacturing technology of composite materials, Automatic Fiber Placement technology (AFP) has combined the advantages of the filament winding technology and Automatic Tape Laying technology (ATL). Moreover the restrictions of them have also be overcome such as “cyclical”, “stability”, “non-bridging” and the “nature path” trajectory design method respectively. With the characteristics of high routing accuracy, good surface flexibility, the continuous variable-angle placement¹, AFP can well suit for manufacturing the complex-shaped composite components with high precision automatically. For example, the fuselage section 19 of A380, the fuselage section 41, 43, 46, 47, 48 of Boeing 787, aft fuselage of V-22, tail boom of UH-60 and the fuselage skin

of F/A-18E/F Super Hornet aircraft all have been manufactured by AFP^{2–5}.

The AFP is a integration technology including the equipment technology, CAD/CAM software technology, and material processing technology¹, in which CAD/CAM technology is the core to achieve the automatization. Trajectory planning, as the key issue of CAD technology, will directly affect the quality of placement process. Summarizing the trajectory planning methods of AFP both at domestic and abroad, four following types will be included: the equidistant path generation method, the fixed angle method with reference lines, the equidistant spiral method, and the fiber steering method based on the stress distribution. The equidistant path generation method^{6–9} is primarily focused on the construction of the initial reference path. Although it is simple and easy to be implemented,

which needn't to analysis the gaps or overlaps between adjacent preprag band, but for complex surface, it's not always effectual to construct an ideal initial reference path. The fixed angle method with reference lines^{10–11} is frequently adopted for revolution surface trajectory planning and architecture the rational reference lines is significant. However fewer reports were found describing the equidistant spiral method and the fiber steering method based on the stress distribution^{12–13}.

Through analyzing the trajectory planning algorithms of AFP domestic and abroad, a novel trajectory design algorithm for the free-form surface with given ply orientation information is proposed. The initial reference path is constructed with the given points and modified fiber-placement directions that are calculated by weighted average algorithm. The full-spreadability solving is applied to the model surface, and all other paths are generated by the parallel equidistant path generation method based on geodesic theory. Finally, the extrapolation-extension

Corresponding author: Wang Peiyuan, postgraduate, major in Automatic Fiber Placement technology, Email: aaa1.5v@163.com

©Smithers Rapra Technology, 2011

operations controlled by Newton-Raphson iteration algorithm on the boundary can satisfy the integrity requirement of boundary placement. Basing on the above algorithms, the CAD module is developed with the environment of CATIA V5R18, and the simulation verifies the validity and effectiveness of this algorithm.

2. THE CONSTRUCTION FOR THE INITIAL REFERENCE PATH

The equidistant path generation method is primarily focused on the construction of the initial reference path because all other center paths are a series of curve families generated from the initial reference path with one band width.

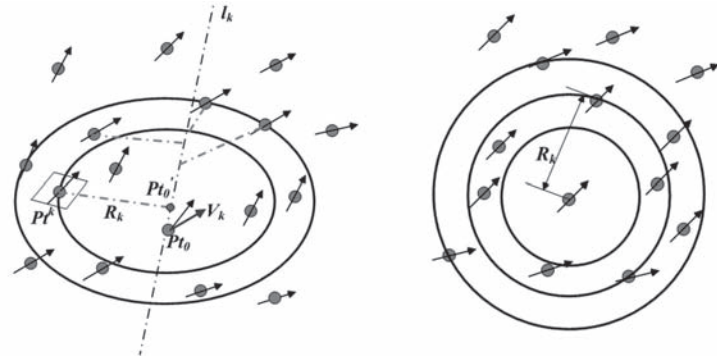
In this study, the ply orientation information, which indicates the loading characteristic and structure optimization requirements, are given in the form of fiber-placement points and the fiber-placement directions within the point area. The initial reference path is constructed through calculating the modified fiber-placement direction on given point with one band width as the weighted range and the given point's reciprocal radius as the weighted factor. This algorithm can summarize all directions in weighted range and calculate a balance result for the placement direction.

2.1 The Calculation of the Modified Fiber-Placement Direction

The model surface is described as $S(u, v) = x(u, v), y(u, v), z(u, v)$, where $(u, v) \in DCR$. $\{Pt^1, Pt^2, \dots, Pt^n\}$ is the point array which indicates the ply orientation information. $Pt_0(x_0, y_0, z_0)$ is the start fiber-placement point. $V_i(x, y, z)$ is the modified direction. The calculating process is described below, see in **Figure 1**.

By the classic differential geometry¹⁴, the normal vector of $Pt_0(x_0, y_0, z_0)$ on $S(u, v)$ can be calculated in Eq.(1):

Figure 1. The calculation of the modified fiber-placement direction



$$e_3^{Pt_k} = \frac{S_u \times S_v}{|S_u \times S_v|} \quad (1)$$

The normal line passing through $Pt_0(x_0, y_0, z_0)$ along the direction $e_3^{Pt_k}$ can be described in Eq.(2):

$$l_k: \frac{x - x_0}{a} = \frac{y - y_0}{b} = \frac{z - z_0}{c} \quad (2)$$

Where a, b, c is the values of $e_3^{Pt_k}$ on three directions.

Taking the valid point $Pt^k(x_k, y_k, z_k) \in \{Pt^1, Pt^2, \dots, Pt^n\}$ in weighted range for example, the vertical plane σ_k passing through point $Pt^k(x_k, y_k, z_k)$ belong to l_k can be constructed in Eq.(3):

$$\sigma_k: a(x - x_k) + b(y - y_k) + c(z - z_k) = 0 \quad (3)$$

Associating the Eq.(2) and Eq.(3), the intersection point $Pt'_0(x'_0, y'_0, z'_0)$ can be obtained, where

$$\begin{aligned} x'_0 &= a \frac{a(x - x_k) + b(y - y_k) + c(z - z_k)}{a^2 + b^2 + c^2} + x_0 \\ y'_0 &= b \frac{a(x - x_k) + b(y - y_k) + c(z - z_k)}{a^2 + b^2 + c^2} + y_0 \\ z'_0 &= c \frac{a(x - x_k) + b(y - y_k) + c(z - z_k)}{a^2 + b^2 + c^2} + z_0 \end{aligned} \quad (4)$$

This space length R_k between points $Pt^k(x_k, y_k, z_k)$ and $Pt'_0(x'_0, y'_0, z'_0)$, which respects the weighted radius in this paper, can be calculated in Eq.(5):

$$R_k = \sqrt{(x_k - x'_0)^2 + (y_k - y'_0)^2 + (z_k - z'_0)^2} \quad (5)$$

Taking the above method, the weighted radius array $\{R_1, R_2, \dots, R_k, \dots, R_n\}$ belong to points $\{Pt^1, Pt^2, \dots, Pt^n\}$ can be obtained. The valid values in $\{R_1, R_2, \dots, R_n\}$ are selected in the range of $R_k \leq W$ (Where W is the band width) and brought them into Eq.(6) to calculate the modified fiber-placement direction $V_{p0}(x, y, z)$ on the start point $Pt_0(x_0, y_0, z_0)$:

$$V_{P_{t_0}}(x, y, z) = \sum_{k=1}^m \frac{1}{R_k} \frac{1}{\sum_{i=1}^m \frac{1}{R_i}} V_{P_{t^k}} \quad (6)$$

Where m is the weighted range valid to the range $R_k \leq W$. R_k and $V_{P_{t^k}}$ are the weighted radius and the fiber-placement direction of point $P_{t^k}(x_k, y_k, z_k)$ respectively.

2.2 The Construction Process of the Initial Reference Path

Taking the modified fiber-placement direction calculated above, the initial reference path can be constructed as follows, see in **Figure 2**.

Firstly, the curvature radius r of point $P_{t_0}(x_0, y_0, z_0)$ can be calculated in Eq.(7)

$$r = |P_{t_0} O_i| = \frac{1}{k_n} \quad (7)$$

Where k_n is the normal curvature on point $P_{t_0}(x_0, y_0, z_0)$.

Then a circle arc is created at point $P_{t_0}(x_0, y_0, z_0)$ along the direction $V_{P_{t_0}}(x, y, z)$ with the radius $r = |P_{t_0} O_i|$. Collect the point $P_{t'_1}$ on this created circle arc and ensure that the arc length between points P_{t_0} and $P_{t'_1}$ is λ (λ is the step length in engineering precision). Project the point $P_{t'_1}$ onto the model surface $S(u, v)$ to obtain the projected point P_{t_1} .

Now taking the point P_{t_1} as the given point and calculated its modified fiber-placement direction $V_{P_{t_1}}$ by Eq.(6).

Repeat all above steps, a points array $\{P_{t_0}, P_{t_1}, \dots, P_{t_n}\}$ along the fiber placement direction can be obtained. Fit all the points in this array to a B-spline and the initial reference path $P(t)$ will be finally constructed, see in **Figure 2**.

3. THE FULL-SPREADABILITY SOLVING OF ALL FIBER PLACEMENT PATHS ON THE MODEL SURFACE

In this part, the amounts of preprag bands lying on two sides of the initial reference path will be calculated to ensure the model surface can be total covered.

Here $P(t)$ is the initial reference path constructed on the model surface. A point array $\{Q_1, Q_2, Q_3, \dots, Q_n\}$ is generated by dispersing the curve $P(t)$. Taking $Q_k \in \{Q_1, Q_2, Q_3, \dots, Q_n\}$ for instance, the tangent vector, normal vector and binormal vector of the discrete-point Q_k can be respectively described as below:

$$\begin{aligned} e_1^{Q_k} &= P'(t) = S_u \frac{du}{dt} + S_v \frac{dv}{dt} \\ e_3^{Q_k} &= \frac{S_u \times S_v}{|S_u \times S_v|} \\ e_2^{Q_k} &= e_1^{Q_k} \times e_3^{Q_k} \end{aligned} \quad (8)$$

Architecture the "feature section" $e_1^{Q_k} \times e_3^{Q_k}$ on the point Q_k , and the intersection-curves $L_1^{Q_k}$ and $L_2^{Q_k}$ lying on the two sides of Q_k are formed by the intersection of the "feature section" with the model surface, see in the **Figure 3**.

The above operations will be applied to all discrete points $\{Q_1, Q_2, Q_3, \dots, Q_n\}$ and

two curve arrays $\{L_1^{Q_1}, L_2^{Q_1}, L_1^{Q_2}, \dots, L_1^{Q_n}\}$ and $\{L_2^{Q_1}, L_2^{Q_2}, L_2^{Q_3}, \dots, L_2^{Q_n}\}$ will be generated. By comparing the arc-length in the above curve arrays respectively, two longest lengths $\max(L_1^{Q_m})$ and $\max(L_2^{Q_m})$ will be obtained, and the amounts of preprag bands lying on two sides of the initial reference path can be calculated by the Eq.(9).

$$\begin{cases} N_1 = \left\lfloor \frac{\max(L_1^{Q_m})}{Nd} \right\rfloor \\ N_2 = \left\lfloor \frac{\max(L_2^{Q_m})}{Nd} \right\rfloor \end{cases} \quad (9)$$

Where N is the amount of tows in a preprag band, d is the diameter of the tow, Nd is one band width of a preprag band, and the symbol $\lfloor \cdot \rfloor$ is the operation of taking the integer-value.

Because geodesic is the most steady line-type between two points on the surface. So the parallel equidistant

Figure 2. The constructed process of initial reference path

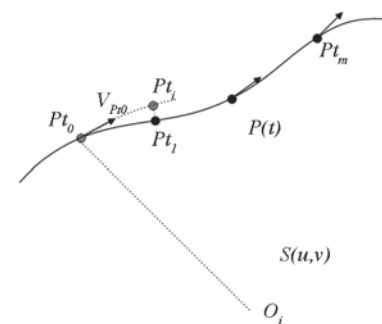
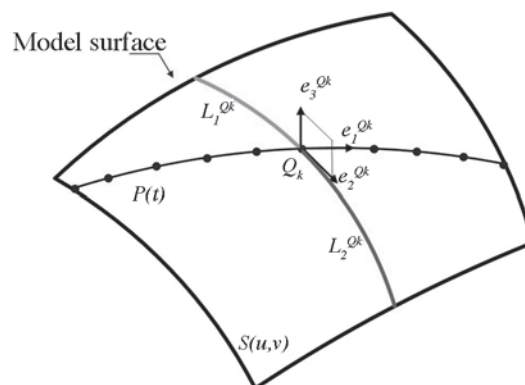


Figure 3. The full-spreadability solving model



path generation method can not only reduce tensile or bending deformation in the placement process, but also slide over the spreadability-analysis issue such as the gaps or overlaps between the adjacent preprag band, which can make the trajectory design simple and feasible.

From the above, all the other paths are generated by the parallel equidistant path generation method^[8] based on geodesic theory until both sides are covered with the fiber placement paths under the amounts of $N_1 = \left\lceil \frac{\max(L_1^{\mathcal{Q}_m})}{nd} \right\rceil$ and $N_2 = \left\lceil \frac{\max(L_2^{\mathcal{Q}_m})}{nd} \right\rceil$ respectively.

4. THE BOUNDARY TREATMENT BY THE NEWTON-RAPHSON ITERATIVE ALGORITHM

The parallel equidistant path generation method is mainly constituted with the offset operations based on the initial reference path in essence. But not all the offset paths can intersect placement boundary and this kind of paths will be extended by extrapolation operation until the intersection occurs. Therefore, how to control the extension length has become a primary content of boundary treatment.

Newton-Raphson algorithm is an iterative method to find the solution of the equation $f(x) = 0$ ¹⁵. Assuming that the implicit equation of the boundary is $B(u(t), v(t))$, the fiber placement trajectory is $P(u(t), v(t))$, and the placement boundaries of $S(u, v)$ can be described in the form of $(u_{\min}, v_{\min} + i\Delta v)$, $(u_{\max}, v_{\min} + i\Delta v)$, $(v_{\min}, u_{\min} + i\Delta u)$, and $(v_{\max}, u_{\min} + i\Delta u)$, where $\Delta v = (v_{\max} - v_{\min})/n$, $\Delta u = (u_{\max} - u_{\min})/n$, $i = 0, 1, \dots, n$, as the **Figure 4** illustrated.

The relative position between the boundary and the trajectory can be described by Eq.(10):

$$f(u(t), v(t)) = B(u(t), v(t)) - P(u(t), v(t)) \quad (10)$$

If the trajectory intersects with the placement boundary, Eq.(10) is sequentially described as Eq.(11):

$$f(u(t), v(t)) = 0 \quad (11)$$

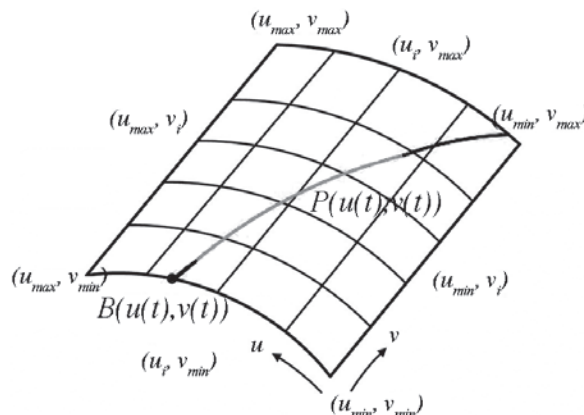
Extrapolate $P(u(t), v(t))$ at both ends with an arc-length of Δl at first, and then Newton-Raphson iterative algorithm is applied to search on the four boundaries by the Eq.(12).

$$(u_{\min}, v_{i+1}) = (u_{\min}, v_i) + \frac{f(u_{\min}, v_i)}{\left(\frac{\partial f}{\partial v_i}\right)_{u=u_{\min}, v=v_i}} \quad (12)$$

Taking the boundary $(u_{\min}, v_{\min} + i\Delta v)$ as the primary iterative area, the iterative results and the related operations are discussed below:

- If the new value (u_{\min}, v_{i+1}) calculated by Eq.(12) calls the equation Eq.(11) into existence, it indicates that one side of $P(u(t), v(t))$ intersects with the placement boundary $(u_{\min}, v_{\min} + i\Delta v)$. Then the other boundaries are continued to traverse in turn with the iteration operation to find whether the intersection occurs at the other side of $P(u(t), v(t))$.
- If the new value (u_{\min}, v_{i+1}) calculated by Eq.(12) cannot call Eq.(11) into existence, so the new value (u_{\min}, v_{i+1}) will be substituted into the Eq.(12) again. This calculation will not stop until the new value (u_{\min}, v_m) , $i+1 < m \leq n$ can call Eq.(11) into existence or the boundary search on $(u_{\min}, v_{\min} + i\Delta v)$ is over.
- If the search on the boundary $(u_{\min}, v_{\min} + i\Delta v)$ is over, and no value can call Eq.(11) into existence, then the traversal moves onto the other boundaries until a new value can all the Eq.(11) into existence.
- If the search on all the boundaries is over, and no value can call the Eq.(11) into existence, the extrapolation operation of $P(u(t), v(t))$ at both ends with an arc-length of Δl will be operated again. Then following steps will turn to (a), (b), and (c) until a new value can all the Eq.(11) into existence.

Figure 4. The boundary treatment model using the Newton-Raphson iterative algorithm



5. ALGORITHM VALIDATION AND SOFTWARE IMPLEMENTATION

With the given ply orientation information in this study, the CAD module is developed by CATIA Automation technology with the environment of CATIA V5R18 to implement the

algorithm above. The **Figure 5** is the algorithm flowchart, the **Figure 6** is the running interface of the CAD module, and the **Figure 7** is the simulation of this trajectory design algorithm.

6. CONCLUSIONS

The traditional fixed-angle trajectory design methods are always easy to

realize, but the loading capability of single ply is weak. It can only meet the force-bearing capability in single direction. Thus the composite structure is always consisted of more layers at the cost of increasing the structure weight. Comparing to the traditional fixed-angle trajectory design method, this study proposes a variable-angle trajectory design algorithm with the

Figure 5. The algorithm flowchart

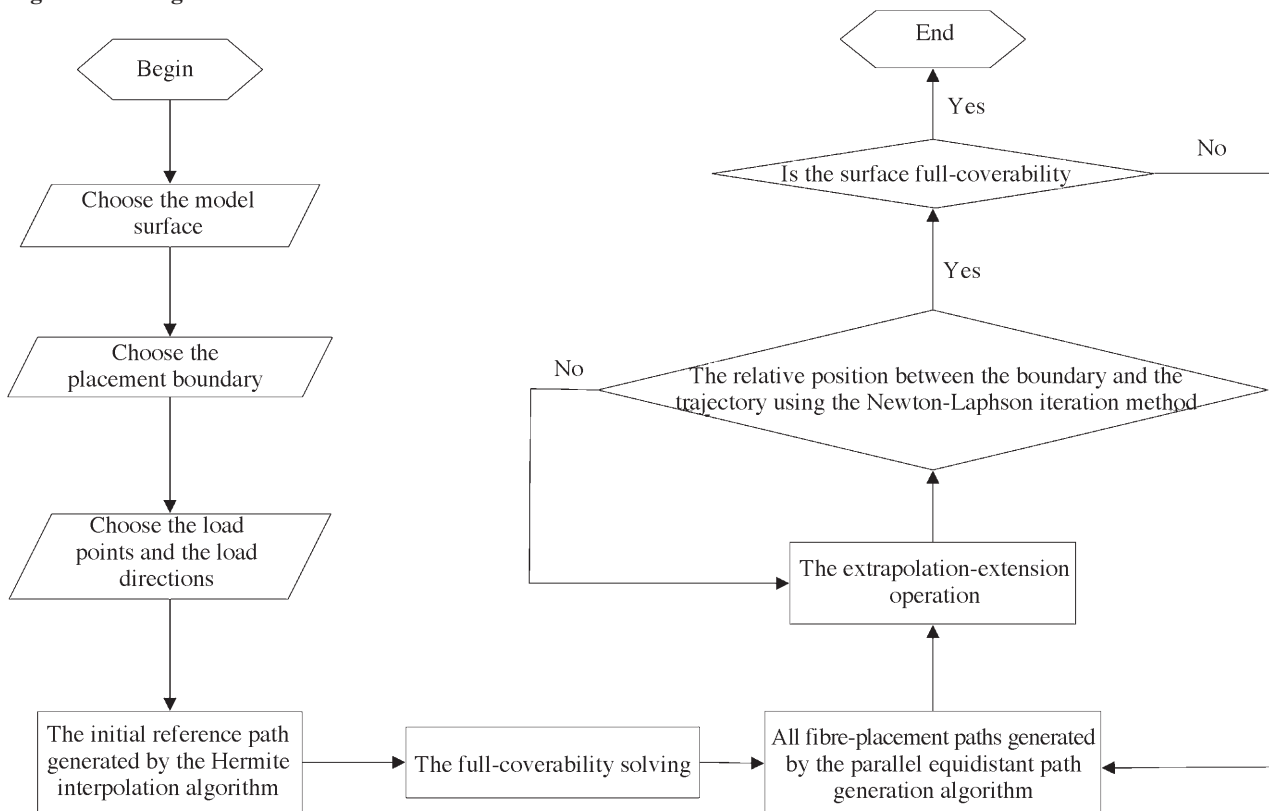


Figure 6. The running interface of the CAD module

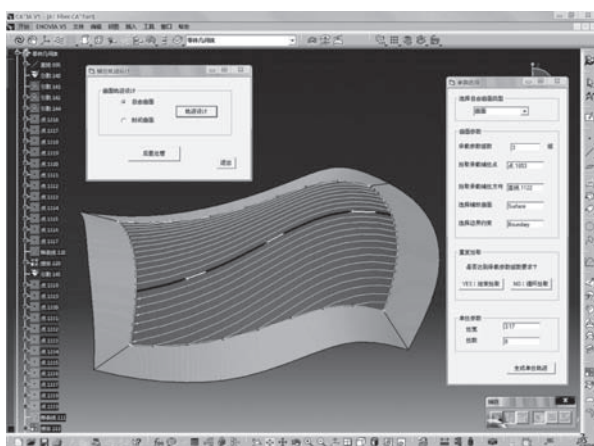
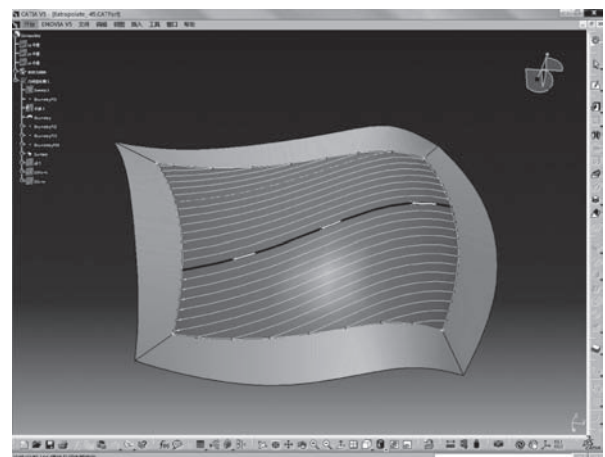


Figure 7. The simulation of this trajectory generation algorithm



ply orientation information which indicates the loading characteristic and optimized requirement. By this ply orientation information, the designed trajectories can show a good loading configuration which can improve the single layer's force-bearing capability in multi-directions and the adaptability in complex loads. This variable-angle trajectory design algorithm can decrease the amounts of layers, reduce the structure weight and give a full play to the advantage of variable angle trajectory design in AFP.

ACKNOWLEDGEMENTS

This work is supported by the national key scientific and technological project, the project No. is 2009ZX04004-102.

REFERENCES

1. Xiao Jun, Li Yong, and Li Jianlong, Application of automatic placement technology on composite component manufacturing of large aircrafts [J], *Aeronautical Manufacturing Technology*, **1** (2008)50~53.
2. Zhang Lihua and Fan Yuqing, The review of composite materials using on aircrafts [J], *Aeronautical Manufacturing Technology*, **3** (2006) 64~66.
3. Bruce Morey, Automating Composites Fabrication [J], *Manufacturing Engineering*, **140(4)** (2008) CT1~CT6.
4. George Marsh, Composites strengthen aerospace hold [J], *Reinforced Plastics*, **46(3)** (2002) 40~43.
5. Lin Sheng, ATL/AFP-The key Machine for Manufacturing of Modern Large Airplane [J], *WMEM*, **5** (2009) 90~95.
6. Bijian Shirinzadeh, Gary Cassidy, Denny Oetomo, et al., Trajectory generation for open-contoured structures in robotic fiber placement [J], *Robotics and Computer-Integrated Manufacturing*, **23** (2007) 380~394.
7. Hale R D, Moon R, Lim K, et al., Integrated design and analysis tools for reduced weight, affordable fiber steered composites [R], Lawrence, Kansas, University of Kansas, 2004.
8. Dang Xudan, Xiao Jun, and Huan Dajun, Implementation on Fiber Placement Parallel Equidistant Path Generation Algorithm [J], *Journal of Wuhan University*, **53(5)** (2007) 613~616.
9. Li Shanyuan, Wang Xiaoping, and Zhu Lijun, Path Planning for Composite Fiber Placement [J], *Aerospace Materials & Technology*, **2** (2009) 25~29.
10. Zhou Yi, An Luling, and Zhou Laishui, Research on Composite Fiber Placement Path Generation Algorithm [J], *Aviation Precision Manufacturing Technology*, **42(2)** (2006) 39~41.
11. Wang Niandong, Liu Yi, and Xiao Jun, Fiber Placement Path Design for Composite Structures in Pipy-Form [J], *Journal of Computer-Aided Design & Computer Graphics*, **20(2)** (2008) 228~233.
12. Shao Guanjun, You Youpeng, and Xiong Hui, Optimal fiber placement paths for free-form surface parts [J], *Journal of Nan jing University of Aeronautics & Astronautics*, **37(S1)** (2005) 144~148.
13. Zeng Wei, Research on Trajectory Generation & Coverability Analysis of Automated Fiber Placement [D], Nanjing, Nanjing University of Aeronautics and Astronautics, 2010.
14. Shi Fazhong, CAGD & NURBS [M], Beijing, Higher Education Press, 1994, 211~251.
15. Liu Weiwen and Li Ge, A Newton-Raphson Method for Geodetic Coordinate Transformation [J], *Computer Simulation*, **23(7)** (2006) 101~104.

Reproduced with permission of the copyright owner. Further reproduction prohibited without permission.